Springer

KSME

Journal of Mechanical Science and Technology 32 (12) (2018) 5823~5829
www.springerlink.com/content/1738-494x(Print)/1976-3824(Online)
DOI 10.1007/s12206-018-1130-8

The influence of material shear nonlinearity on multidirectional laminates in terms of failure envelopes †

Hongli Jia[1], Hyun-Ik Yang[2,*] and Tae-won Kang[2]

[1]*Department of Mechanical Engineering, Hanyang University, Ansan 15588, Korea*
[2]*Department of Mechanical Design, Hanyang University, Ansan 15588, Korea*

(Manuscript Received May 30, 2018; Revised September 27, 2018; Accepted October 8, 2018)

Abstract

Influence of material shear nonlinearity on multidirectional laminates in terms of failure envelopes was investigated. In applying classic laminate theory, elastic constants were employed in transverse and longitudinal directions, while initial shear modulus was substituted by the secant shear modulus, which was achieved by means of Ramberg-Osgood model. The fracture curves were generated from maximum stress, Tsai-Wu and Puck criteria. The similarities and differences between nonlinear and linear shear models can be expressed in terms of symmetric balanced laminates $[\pm\theta^\circ]_{2s}$ and asymmetric laminates $[0^\circ_2/\pm\theta^\circ]$, which are both arranged by material E-glass/MY750 oriented at different directions. All σ_1 - σ_2 failure envelopes due to material nonlinearity extend outward in tensile and compressive directions, but the phenomenon is not obvious with increasing ply angles. Similarly, the differences of all σ_1 - τ_{12} failure envelopes between nonlinear shear analysis and linear shear analysis are decreasing with increased ply angles. Ply orientations and loading directions are involved in the effect of nonlinear shear properties on failure envelopes. According to the failure modes obtained from maximum stress criterion, it is reasonably derived that the influence of material shear nonlinearity will lead whether the failure envelopes from the other two failure criteria are more conservative or not.

Keywords: Failure envelopes; GFRP; Nonlinear shear property; Ramberg-Osgood model

1. Introduction

A composite material can be manufactured when orthotropic elastic fibers are embedded into a plate isotropic elastoplastic matrix. However, due to poor properties in transverse direction compared with properties in longitudinal direction, plies cannot be aligned parallel to the fiber direction, Hence, plies oriented at different directions are arranged into the laminate in order to achieve desired strength and stiffness. From experimental stress-strain curves [1], it can be observed that uniaxial stress-strain curves are linear and shear stress-strain is significantly nonlinear for unidirectional laminates (UD) when uniaxial loads are applied. While UD are subjected to the loads with off-axis angle other than 0°, obvious nonlinear stress-strain response governs [2]. For multidirectional laminates [3, 4], both uniaxial and shear stress-strain curves show nonlinear relationships; however, uniaxial stress-strain curves of laminates composed of plies oriented at a small angle may propose a slightly nonlinear property at a high strain level, while shear response is always nonlinear no matter what laminate stacked sequences.

Based on the characteristics mentioned above, many researchers have studied the influence of nonlinear properties on mechanical behavior of laminates. In Ref. [5], tensile and shear strengths of UD are investigated by means of Puck's action plane in terms of improved nonlinear model, and there also exists good agreement between force-displacement and curves of experimental results. As for the effect of material nonlinearity on compressive strength of laminates, it turns out to reduce the predicted value of the strength through the utilization of a kind band model [6]. Zand [7] improved a strain energy based failure theory to predict the mechanical response and failure of laminates considering a nonlinear inelastic material. And the model shows better agreement between numerical results and experimental data for laminates than angle ply laminates. In this paper, the influence of material shear nonlinearity on failure envelopes of multidirectional laminates is presented.

2. Theory

2.1 Nonlinear shear stress-strain constitutive relation

Generally, material elastic constants are employed in analysis of composite laminates. Initial modulus remains constant

*Corresponding author. Tel.: +82 314368150, Fax.: +82 314368150
E-mail address: skynet@hanyang.ac.kr
† Recommended by Associate Editor Kyeongsik Woo

Table 1. Ramberg-Osgood parameters for E-glass/MY750 material.

Initial shear modulus G_0 (GPa)	5.83
Shear asymptotic stress τ_0 (MPa)	76.8
Shear parameter n	2

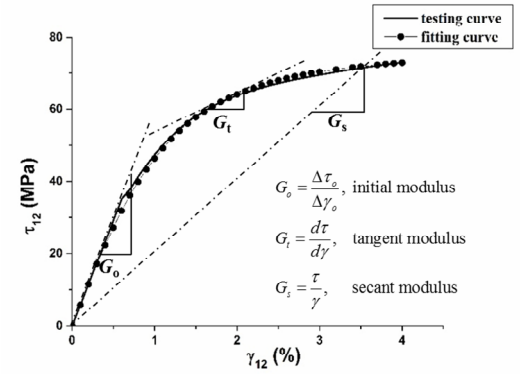

Fig. 1. The definition of elastic moduli and comparison of experimental and fitting curves for E-glass/MY750 UD.

throughout the whole proceeding of increasing or decreasing loads. However, this is different than the reliably experimental results, just shown in Fig. 1. Regardless of ply orientations or load conditions, shear stress-strain curves are always significantly nonlinear owing to plasticity in the matrix. Aiming at fitting the in-plane shear stress-strain experimental curves, both macro-mechanical and micro-mechanical models are proposed [8-11]. In the process, difficulties lie in the area where the slope of stress strain curves changes obviously.

However, the Ramberg-Osgood model can provide material elastoplastic responses at a low strain level. And it is proposed by two different expressions that strains and stresses are regarded as variables, respectively. From the stress-strain curve depicted in Fig. 1, stress slightly increases at a high strain level. Furthermore, it may have an asymptotic valve with being close to the failure strain. Hence, in order to achieve match accuracy, the format described in the Eq. (1) is taken into account. Both secant and tangent moduli can bring a good agreement between numerical analysis and test data. But just as the definition of elastic moduli, shown in Fig. 1, the secant modulus is advantageous on simple calculations over the tangent modulus. Therefore, secant shear modulus is used for accurate shear stress-strain relations instead of initial shear modulus or tangent modulus, written in Eq. (2).

$$\tau_{12} = \frac{G_0\gamma_{12}}{\left(1+\left(\frac{G_0\gamma_{12}}{\tau_0}\right)^n\right)^{\frac{1}{n}}}, \tag{1}$$

$$G_S = \frac{G_0}{\left(1+\left(\frac{G_0\gamma_{12}}{\tau_0}\right)^n\right)^{\frac{1}{n}}}. \tag{2}$$

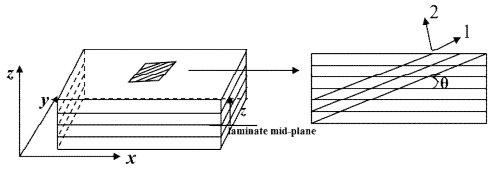

Fig. 2. Schematic of definitions of mid-plane and the ply angle.

The Ramberg-Osgood coefficients involved in the expressions are summarized in Table 1. Fig. 1 shows a good agreement between experimental data [1] and fitting curves for material E-glass/MY750 through the formula.

Principal material direction is not always coincident with laminate direction, since all plies oriented in fiber direction could not always exist due to poor transverse properties. Consequently, a rotation angle θ is made from material coordinate system (1, 2, 3) to laminate coordinate system (x, y, z) when material coordinates are not parallel to the loading direction, just presented in Fig. 2.

In the analysis, *Kirchhoff hypothesis* is performed. So transverse normals do not change in lengths (i.e., $\varepsilon_z = 0$), and remain straight and perpendicular to the middle surface after deformation ($\gamma_{yz} = \gamma_{xz} = 0$). Accordingly, the constitutive law for plane stress condition is defined with transformation matrix.

$$\begin{Bmatrix}\sigma_x\\ \sigma_y\\ \tau_{xy}\end{Bmatrix} = \left[\overline{Q}\right]\begin{Bmatrix}\varepsilon_x\\ \varepsilon_y\\ \gamma_{xy}\end{Bmatrix} = \begin{bmatrix}\overline{Q}_{11} & \overline{Q}_{12} & \overline{Q}_{16}\\ \overline{Q}_{12} & \overline{Q}_{22} & \overline{Q}_{26}\\ \overline{Q}_{16} & \overline{Q}_{26} & \overline{Q}_{66}\end{bmatrix}\begin{Bmatrix}\varepsilon_x\\ \varepsilon_y\\ \gamma_{xy}\end{Bmatrix}, \tag{3}$$

where $\overline{Q}$ is modified stiffness matrix specified by reduced stiffness matrix and transformation matrix. The elements in $\overline{Q}$ are listed below.

$$\begin{aligned}
\overline{Q}_{11} &= m^4Q_{11} + 2m^2n^2Q_{12} + n^4Q_{22} + 4m^2n^2Q_{66}\\
\overline{Q}_{12} &= m^4Q_{12} + m^2n^2\left(Q_{11}+Q_{22}\right) + n^4Q_{22} - 4m^2n^2Q_{66}\\
\overline{Q}_{16} &= mn\left[m^2\left(Q_{11}-Q_{12}\right) + n^2\left(Q_{12}-Q_{22}\right) - 2\left(m^2-n^2\right)Q_{66}\right]\\
\overline{Q}_{22} &= m^4Q_{22} + 2m^2n^2Q_{12} + n^4Q_{11} + 4m^2n^2Q_{66}\\
\overline{Q}_{26} &= mn\left[m^2\left(Q_{12}-Q_{22}\right) + n^2\left(Q_{11}-Q_{12}\right) + 2\left(m^2-n^2\right)Q_{66}\right]\\
\overline{Q}_{66} &= m^2n^2\left(Q_{11}-Q_{12}\right) - m^2n^2\left(Q_{12}-Q_{22}\right) + \left(m^2-n^2\right)^2Q_{66}\\
m &= \cos\theta, n = \sin\theta, Q_{11} = 1/E_1, Q_{12} = -\nu_{12}/E_1, Q_{66} = 1/G_S.
\end{aligned}$$

It is easily concluded that the utilization of secant shear modulus reduces coefficients $\overline{Q}_{11}$, $\overline{Q}_{22}$, $\overline{Q}_{66}$ and increases coefficient $\overline{Q}_{12}$. A positive effect on $\overline{Q}_{16}$ occurs when the effect on $\overline{Q}_{26}$ is negative, and a negative effect on $\overline{Q}_{16}$ occurs when the effect on $\overline{Q}_{26}$ is positive. The two parameters $\overline{Q}_{16}$ and $\overline{Q}_{26}$ could play a significant role in shear extension coupling effect between the resultant stress and strain, which makes analysis stress and deformation analyses more complicated. However, in-plane shear property makes no contribu-

tion to components $\bar{Q}_{16}$, $\bar{Q}_{26}$, $\bar{Q}_{66}$ in transforming reduced stiffness if the ply is aligned at 45°. The previous parameters $\bar{Q}_{ij}$ are used for calculating in-plane resultant forces per unit width {N} and moments per unit width {M} in terms of mid-plane strains ε^0 and plate curvatures κ^0.

$$\begin{Bmatrix} N \\ M \end{Bmatrix} = \begin{bmatrix} A & B \\ B & D \end{bmatrix} \begin{Bmatrix} \varepsilon^0 \\ \kappa \end{Bmatrix}, \tag{4}$$

where [A], [B] and [D] are extensional stiffness matrix, coupling stiffness matrix, bending stiffness matrix, respectively.

2.2 Criteria for failure mechanisms

Failure envelopes are generated by combination of the stresses acting on laminates and material conventional strengths in a certain criterion. There is no failure theory to solve all load conditions. Therefore, in this study, three typical kinds of failure criteria were employed in observing the influence of nonlinear shear behavior on the failure envelopes: Maximum stress failure criterion, a limit failure model; Tsai-Wu failure criterion, an interactive failure model; Puck failure criterion, a separate mode. All three theories are based on first ply failure.

Based on maximum stress theory, failure occurs when any one of the lamina stresses equals or exceeds the corresponding ultimate strength. The function is written below.

$$\begin{aligned} &X_C < \sigma_1 < X_T \\ &Y_C < \sigma_2 < Y_T \\ &-S_{12} < \tau_{12} < S_{12}\,. \end{aligned} \tag{5}$$

Tsai-Wu criterion is proposed by a series of quadratic polynomial expressions involving all stress components, which are formulated to match experimental results physically. The function for plane stress condition can be written below.

$$F = F_{11}\sigma_1^2 + F_{22}\sigma_2^2 + F_{66}\tau_{12}^2 + 2F_{12}\sigma_1\sigma_2 + F_1\sigma_1 + F_2\sigma_2\,. \tag{6}$$

Like the Tsai-Wu failure criterion, the Puck criterion is also based on a phenomenological model, but the Puck criterion distinguishes between fiber and matrix for failure, which is divided into tension and compression modes, separately [12, 13].

Fiber tensile failure ((…) > 0):

$$\frac{1}{\varepsilon_{1T}}\left(\varepsilon_1 + \frac{v_{f12}}{E_{f1}} m_{\sigma f}\sigma_2\right) = 1\,. \tag{7a}$$

Fiber compressive failure ((…) < 0):

$$\frac{1}{\varepsilon_{1C}}\left|\varepsilon_1 + \frac{v_{f12}}{E_{f1}} m_{\sigma f}\sigma_2\right| + \left(10\gamma_{12}\right)^2 = 1 \text{ for } \left(\ldots\right) < 1\,. \tag{7b}$$

Matrix tensile failure ($\sigma_2 > 0$):

$$\sqrt{\left(\frac{\tau_{12}}{S_{12}}\right)^2 + \left(1 - p_{\perp\|}^{(+)}\frac{Y_T}{S_{12}}\right)\left(\frac{\sigma_2}{Y_T}\right)^2} + p_{\perp\|}^{(+)}\frac{\sigma_2}{Y_T} = 1\,. \tag{7c}$$

Matrix compressive failure ($\sigma_2 < 0, 0 \le \left|\frac{\sigma_2}{\tau_{12}}\right| \le \frac{R_{\perp\perp}^A}{|\tau_{21c}|}$):

$$\frac{1}{S_{12}}\left(\sqrt{\tau_{12}^2 + \left(p_{\perp\|}^{(-)}\sigma_2\right)^2} + p_{\perp\|}^{(-)}\sigma_2\right) = 1 \text{ if } 0 \le \left|\frac{\sigma_2}{\tau_{12}}\right| \le \frac{R_{\perp\perp}^A}{|\tau_{21c}|}\,. \tag{7d}$$

Matrix compressive failure ($\sigma_2 < 0, 0 \le \left|\frac{\tau_{12}}{\sigma_2}\right| \le \frac{|\tau_{21c}|}{R_{\perp\perp}^A}$):

$$\left[\left(\frac{\tau_{12}}{2\left(1 + p_{\perp\perp}^{(-)}S_{12}\right)}\right)^2 + \left(\frac{\sigma_2}{Y_C}\right)^2\right]\frac{Y_C}{-\sigma_2} \text{ if } 0 \le \left|\frac{\tau_{12}}{\sigma_2}\right| \le \frac{|\tau_{21c}|}{R_{\perp\perp}^A}, \tag{7e}$$

where X_T, X_C, Y_T, Y_C and S_{12} are strengths corresponding to longitudinal, transverse and shear directions, respectively. All strengths take absolute values, while all stresses keep their signs. The coefficients used in the Tsai-Wu formula are determined by the material conventional strengths, which are listed in the following.

$$F_{11} = \frac{1}{X_T X_C}, F_{22} = \frac{1}{Y_T Y_C}, F_{66} = \frac{1}{S_{12}^2}, F_{12} = -\frac{1}{2\sqrt{X_T X_C Y_T Y_C}}$$
$$F_1 = \frac{1}{X_T} - \frac{1}{X_C}, F_2 = \frac{1}{Y_T} - \frac{1}{Y_C}\,.$$

As for coefficients used in Puck criterion, $p_{\perp\|}^{(+)}$ and $p_{\perp\|}^{(-)}$ are inclination parameters derived from experimental (σ_2, τ_{12}) fracture curves. Other parameters $R_{\perp\perp}^A$, $p_{\perp\perp}^{(-)}$ and τ_{12c} are obtained below. Index θ is fracture angle defined by the angle between normal direction of fracture plane and transverse direction of lamina.

$$\sigma_n = \sigma_2\cos^2\theta, \tau_{nt} = -\sigma_2 \sin\theta\cos\theta, \tau_{nl} = \tau_{12}\cos\theta,$$
$$R_{\perp\perp}^A = \frac{S_{12}}{2p_{\perp\|}^{(-)}}\sqrt{1 + 2p_{\perp\|}^{(-)}\frac{Y_C}{S_{12}}} - 1, p_{\perp\perp}^{(-)} = p_{\perp\|}^{(-)}\frac{R_{\perp\perp}^A}{S_{12}}, \tau_{12c} = S_{12}\sqrt{1 + 2p_{\perp\perp}^{(-)}}\,.$$

2.3 Methods for generating failure envelopes

Biaxial combining loads are applied to observe the effect of shear nonlinear behavior on the failure of multidirectional laminates. The fracture curves are generated for all possible stress combinations, which are caused by the following three types of load combinations for the flat plates: *Nx - Ny*, *Nx-Nxy*, and *Ny - Nxy*, as shown in Fig. 3.

Detailed algorithm to generate failure envelopes is presented in Fig. 4. According to the flowchart, Fig. 5 shows an example of σ_1 - τ_{12} curves for UD E-glass/MY750. In the process of getting the curve, the first step is to find the coordi-

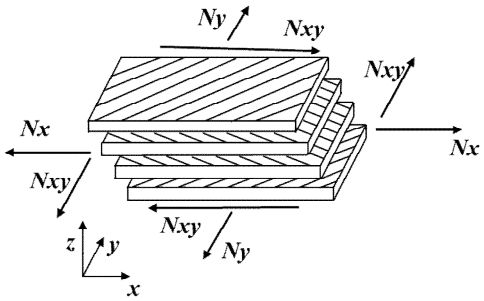

Fig. 3. In-plane loads per unit length on a composite plate.

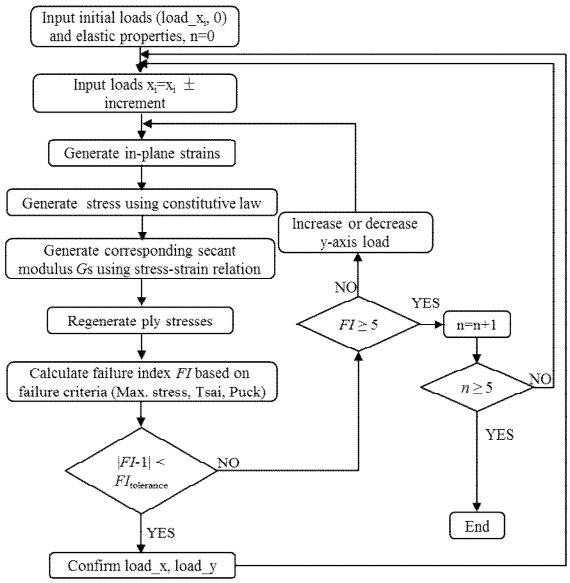

Fig. 4. Computational algorithm for generating failure envelopes.

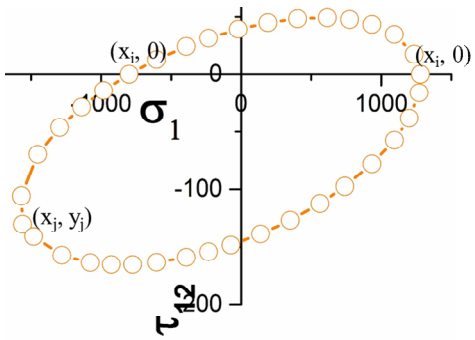

Fig. 5. σ_1-τ_{12} curves for UD E-glass/MY750 obtained by computational algorithm described in Fig. 4.

nates of failure loads of laminates on x - axis, (x_i, 0). The next step is to confirm the critical values (x_j, y_j). As a result, the range of x - axis coordinates is identified. So for any x - axis value selected in the range, y - axis values can be adjusted to meet that the failure index *FI* is in the tolerance range.

Without consideration of material shear nonlinearity, the failure stresses can be calculated by equation $N_i/(FI \cdot t)$. *FI* is the failure index generated from the above three criteria. Condition FI < 1 defines the safe zone of the stress states for the

Table 2. Material properties of E-glass/MY750.

Elastic properties		Strength properties		Puck criterion	
E_1(GPa)	45.6	X_T (MPa)	1280	E_{f1} (GPa)	76.8
E_2(GPa)	16.2	X_C (MPa)	800	ν_{f12}	0.2
ν_{12}	0.278	Y_T (MPa)	40	$m_{\sigma f}$	1.3
G_{12}(GPa)	5.83	Y_C (MPa)	145	$p_{\perp\parallel}^{(+)}$	0.3
		S_{12} (MPa)	73	$p_{\perp\parallel}^{(-)}$	0.25

Table 3. Summary of laminate types and plots required.

Case No.	Laminate lay-up	Plots required		
1	[±30°]2s	σ_1 vs σ_2	σ_1 vs τ_{12}	-
2	[±45°]2s	σ_1 vs σ_2	σ_1 vs τ_{12}	
3	[±60°]2s	σ_1 vs σ_2	σ_1 vs τ_{12}	
4	[0°$_2$/±30°]	σ_1 vs σ_2	σ_1 vs τ_{12}	σ_2 vs τ_{12}
5	[0°$_2$/±45°]	σ_1 vs σ_2	σ_1 vs τ_{12}	σ_2 vs τ_{12}
6	[0°$_2$/±60°]	σ_1 vs σ_2	σ_1 vs τ_{12}	σ_2 vs τ_{12}
Thickness of ply is 0.125 mm				

laminates. And the area enclosed by the failure lines means a safe zone. As long as stress states are ranged in the safe zone, material can still sustain from increasing load. In our study, the tolerance $FI_{tolerance}$ is 0.03, which means the secant modulus keeps constant when the equation occurs |FI-1| < $FI_{tolerance}$. In other words, the material property is assumed linear when the distance of |FI-1| is less than $FI_{tolerance}$ value.

3. Numerical results

The material E-glass/MY750 properties including elastic properties, strength and parameters for Puck's criterion are listed in Table 2.

There are two different kinds of laminate stacked sequences [±θ°]2s, [0°/±θ°] employed, in which θ° varies among 30°, 45°, 60°. The laminates arranged with [±θ°]2s are symmetric balanced material. There should be an identical ply at position with negative thickness direction when the ply in θ° direction is arranged at position with positive thickness direction. Hence, there is no connection between in-plane forces and out-of-plane deformation of laminates, and in-plane strains are also irrelevant to moments. Moreover, balanced laminates are constituted of equal numbers of θ° and -θ° angled plies, which leads to no coupling between axial loads and in-plane shear strain. The required plots and laminates layup are summarized in Table 3.

In this section, the influence of nonlinear shear stress-strain property on fracture curves resulting from the three failure criteria is compared in Figs. 6 and 7, followed by the legend of the figures. Therein, the σ_2 vs τ_{12} envelopes from [±30°]2s and [±60°]2s laminates have physically the same meaning for σ_1 vs τ_{12} envelopes from [±60°]2s and [±30°]2s laminates, which leads to that σ_2 vs τ_{12} envelopes can be neglected.

As shown from the failure envelopes for symmetrical bal-

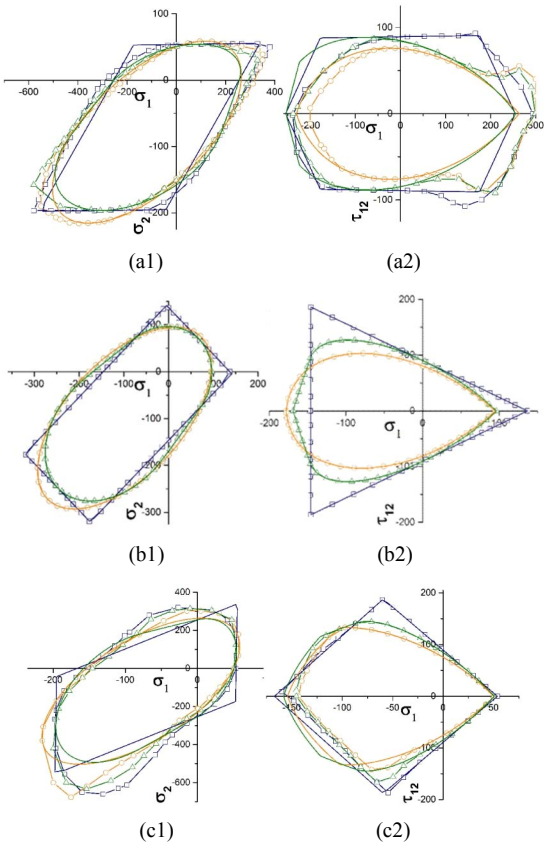

Fig. 6. Comparison of failure envelopes between linear and nonlinear shear responses for $[\pm\theta^\circ]_{2S}$ E-glass/MY750: (a1) σ_1-σ_2 for $[\pm30^\circ]_{2S}$; (a2) σ_1-τ_{12} for $[\pm30^\circ]_{2S}$; (b1) σ_1-σ_2 for $[\pm45^\circ]_{2S}$; (b2) σ_1-τ_{12} $[\pm45^\circ]_{2S}$; (c1) σ_1-σ_2 for $[\pm60^\circ]_{2S}$; (c2) σ_1-τ_{12} for $[\pm60^\circ]_{2S}$.

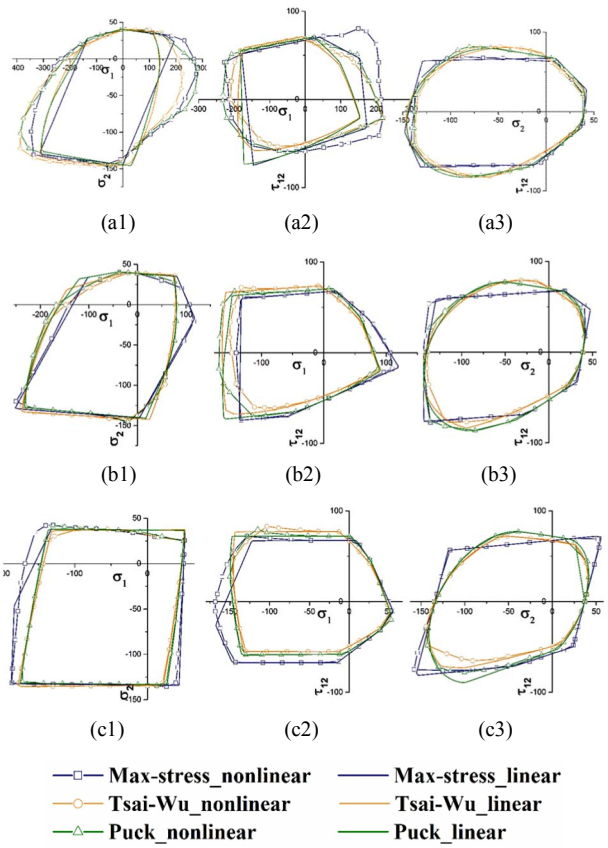

Fig. 7. Comparison of failure envelopes between linear and nonlinear shear responses for $[0^\circ_2/\pm\theta^\circ]$ E-glass/MY750: (a1) σ_1-σ_2 for $[0^\circ_2/\pm30^\circ]$; (a2) σ_1-τ_{12} for $[0^\circ_2/\pm30^\circ]$; (a3) σ_2-τ_{12} for $[0^\circ_2/\pm30^\circ]$; (b1) σ_1-σ_2 for $[0^\circ_2/\pm45^\circ]$; (b2) σ_1-τ_{12} for $[0^\circ_2/\pm45^\circ]$; (b3) σ_2-τ_{12} for $[0^\circ_2/\pm45^\circ]$; (c1) σ_1-σ_2 for $[0^\circ_2/\pm60^\circ]$; (c2) σ_1-τ_{12} for $[0^\circ_2/\pm60^\circ]$; (c3) σ_2-τ_{12} for $[0^\circ_2/\pm60^\circ]$.

anced laminates resulting from Fig. 6, the following observations can be made. 1) For all curves of $[\pm45^\circ]_{2s}$ laminates, there is no difference of curves between nonlinear analysis and linear analysis. Checking variation of elements in the transformed stiffness matrix, the in-plane shear property has no contribution to the shear property of laminates. Hence, failure stress is also not influenced when biaxial loads are applied. 2) For σ_1 vs σ_2 curves of $[\pm30^\circ]_{2s}$ laminates, stress components σ_1 extend outward in x - axis tensile and compressive directions. 3) For those curves of $[\pm60^\circ]_{2s}$ laminates, stress components σ_1 extend outward in y - axis tensile and compressive directions. 4) For σ_1 vs τ_{12} curves of $[\pm30^\circ]_{2s}$ laminates, all curves from linear analysis are more conservative than those from nonlinear analysis when laminates are just under tensile loads ($\sigma_1>0$). Meanwhile, curves from nonlinear analysis are more conservative than those from linear analysis when laminates are just under tensile loads ($\sigma_1<0$). 5) for σ_1 vs τ_{12} curves of $[\pm60^\circ]_s$ laminates, curves almost coincide comparing the nonlinear shear influences under tensile loads ($\sigma_1 > 0$); curves with regard to nonlinearity show fewer safe zones except that endpoints of curves are a little higher.

The influence of material shear nonlinearity on failure envelopes for $[0^\circ_2/\pm\theta^\circ]$ is depicted in Fig. 7. Out-of-plane deformation occurs when in-plane forces are applied because of asymmetry of the laminates, which leads to the irregular fracture curves. As a consequence, the following observations can be made. 1) For σ_1 vs σ_2 curves of $[0^\circ_2/\pm\theta^\circ]$ (θ° = 30°, 45°, 60°) laminates, except that the closed curves of $[0^\circ_2/\pm30^\circ]$ with regard to material shear nonlinearity cover the conservative curves from linear analysis, curves from the two different models coincide for the other two different stacked laminates. To be more precise, only stress components σ_1 from $[0^\circ_2/\pm30^\circ]$ laminates just extend outward in x – axis tensile and compressive directions. 2) For σ_1 vs τ_{12} curves of $[0^\circ_2/\pm\theta^\circ]$ laminates, the differences of all σ_1 - τ_{12} failure envelopes between nonlinear shear analysis and linear shear analysis are decreasing with increasing ply angles. Especially, shear nonlinearity does not affect the fracture curves at all for $[0^\circ_2/\pm60^\circ]$ material. 3) For σ_2 vs τ_{12} curves of $[0^\circ_2/\pm\theta^\circ]$ laminates, there is nearly no difference between nonlinear shear analysis and linear shear analysis.

4. Discussion and conclusions

All trends of failure envelopes described by arbitrary stress combinations resulting from the three failure criteria are the

same, that is, curves from the other two criteria also present more safe zone when failure curves from any one of the three criteria cover more safe zone in terms of material shear nonlinear property.

In this study, secant shear modulus rather than initial shear modulus was employed in the generation of failure envelopes when laminates are under biaxial loads; thus, the decrement in shear modulus results in the decreasing diagonal values of the ABD matrix, which brings about increment in absolute values of strains and curvatures acting on reference plane. Lamina strains are derived from reference plane strains and curvatures. Consequently, strain distributions of any ply embedded in laminates are accordance with strain components resulting from left plies for symmetric balanced laminates, while strain behaviors of asymmetrical laminates could not be like this.

For symmetrical balanced laminates, stress components of ply oriented in positive direction should be the same in magnitude and sign as the corresponding stresses components of ply oriented in negative direction. In addition, stresses acting on the lower surface should be the same as the stresses acting on the upper surface of the identical ply. However, the stress distribution rules mentioned above would not apply at all to the asymmetrical laminates. Stress components of any one of the three plies are different from the corresponding stress components of any one of the left two plies. And the bottom stresses are not equal to the top corresponding stresses of the same layer. It is all due to the existence of a coupling stiffness matrix in asymmetrical laminates.

Due to the changes in stiffness matrix, the stress states causing nonlinear numerical model failure may not be the same as the stress states causing linear numerical model failure, even when loads are the same in direction and magnitude. It is shown clearly in Fig. 1(b) that the larger shear strain provides more influence on the secant modulus. Failure occurs when any separate item of combined stresses reaches the conventional strength of ply embedded in laminates based on maximum stress criterion.

For symmetric balanced laminates, decrement of shear modulus leads to that the maximum absolute values of axial stresses (σ_1 and σ_2) are increased and that maximum absolute values of in-plane shear stresses (τ_{12}) are decreased. Whether normal stress or shear stress causes the linear model failure, as long as it is shear stress that causes the nonlinear shear model based on maximum stress criterion, which will lead that the nonlinear model with smaller value of shear stress needs the larger values of normal stress to make up, in order to make the failure indexes from the other two criteria equal to 1. When normal stress causes the two models failure, it means that the influence of secant shear modulus on stresses is limited. When normal stress causes the nonlinear model failure and shear stress causes the linear model failure, it means the shear stress of nonlinear model has a smaller value. The conditions mean that the nonlinear shear model provides more conservative failure envelopes Therefore, once which stress component causes fracture is determined according to maximum stress criterion, the similarity and differences of failure envelopes between the nonlinear shear models resulting from Tsai-Wu and Puck criteria can be derived. Failure envelopes of [±45°]2s laminates from the nonlinear model are the same as those from the linear model, because shear nonlinearity makes no contribution to ply stress components owing to expressions of $\bar{Q}_{ij}$.

For asymmetric laminates, the fracture of the nonlinear and linear shear models could be caused by the lamina placed in the same orientation and position, but it is also possible that the fracture of the two models is caused by the lamina placed in the inconsistency of orientation and position. However, the content in the previous paragraph described by different stress components causing laminates failure will lead to the fact that similarity and differences of failure envelopes from the two models can be applied here.

The failure mentioned in our study is the initial failure, which means one lamina of the laminate fractures, but the load capability of the laminate is determined by the final ply failure derived from a progressive failure analysis model lacked in the study. From the comparison of failure envelopes presented in the above figures and discussions, the facture stresses of failed plies in sequence and the failure models from the nonlinear shear analysis could not be the same as the conditions from the linear shear analysis under the same given load, which leads to different theoretical stress-strain curves of laminates resulting in different predictions of load capability.

References

[1] P. D. Soden, M. J. Hinton and A. S. Kaddour, Lamina properties, lay-up configurations and loading conditions for a range of fibre reinforced composite laminates, *Composite Science and Technology*, 58 (7) (1998) 1011-1022.

[2] J. Andersons, J. Modniks and E. Sparnins, Modeling the nonlinear deformation of flax-fiber-reinforced polymer matrix laminates in active loading, *J. of Reinforced Plastics and Composites*, 34 (3) (2015) 248-256.

[3] S. Ogihara, S. Kobayashi and K. L. Reifnider, Characterization of nonlinear behavior of carbon/epoxy unidirectional and angle-ply laminates, *Advanced Composite Materials,* 11 (3) (2003) 239-254.

[4] T. Yokozeki, T. Ogasawara and T. Ishikawa, Nonlinear behavior and compressive strength of unidirectional and multidirectional carbon fiber composite laminates, *Composites Part A: Applied Science and Manufacturing,* 37 (11) (2006) 2069-2079.

[5] T. Kroupa, V. Laš and R. Zemčík, Improved nonlinear stress-strain relation for carbon-epoxy composites and identification of material parameters, *J. of Composite Materials*, 45 (9) (2011) 1045-1057.

[6] T. Yokozeki, T. Ogasawara and T. Ishikawa, Effects of the fiber nonlinear properties on the compressive strength prediction of unidirectional carbon–fiber composites, *Composite Science and Technology*, 65 (14) (2005) 2140-2147.

[7] Zand Behrad, Modelling of composite laminates subjected to multiaxial, *Doctoral Dissertation*, Ohio State University (2007) Retrieved from https://etd.ohiolink.edu/.

[8] W. P. Lin and H. T. Hu, Nonlinear analysis of fiber-reinforced composite laminates subjected to uniaxial tensile load, *J. of Composite Materials*, 36 (12) (2002) 1429-1450.

[9] F. Hassani, M. M. Shokrieh and L. B. Lessard, A fully non-linear 3D constitutive relationship for the stress analysis of a pin-loaded composite laminate, *Composite Science and Technology*, 62 (3) (2002) 429-439.

[10] C. T. Sun and J. L. Chen, A micromechanical model for plastic behavior of fibrous composites, *Composite Science and Technology*, 40 (2) (1991) 115-129.

[11] R. Haj-Ali and H. Kilic, Nonlinear constitutive models for pultruded FRP composites, *Mechanics of Materials*, 35 (8) (2003) 791-801.

[12] A. Puck and H. Schürmann, Failure analysis of FRP laminates by means of physically based phenomenological models. *Composite Science and Technology*, 58 (7) (1998) 1045-1068.

[13] A. Puck, J. Kopp and M. Knops, Guidelines for the determination of the parameters in Puck's action plane strength criterion, *Composite Science and Technology*, 62 (3) (2002) 371-378.

Hyun Ik Yang, Ph.D., is a Professor in the Dept. of Mechanical Engineering of College of Engineering Science ERICA Hanyang University. He received Ph.D. in Mechanical Engineering from Columbia University in the City of New York.